Correlating Pyrene Excimer Formation with Polymer Chain Dynamics in Solution. Possibilities and Limitations

Mark Ingratta and Jean Duhamel*

Institute for Polymer Research, Department of Chemistry, University of Waterloo, 200 University Avenue West, Waterloo, ON N2L 3G1, Canada

Received February 12, 2007; Revised Manuscript Received May 28, 2007

ABSTRACT: Four types of pyrene-labeled polystyrene samples (Py−PS) were prepared and the process of excimer formation between the pyrene labels was characterized by steady-state and time-resolved fluorescence to assess the effect the mode of pyrene incorporation into a polymer has on the kinetics of excimer formation. The pyrene label was incorporated into the PS backbone by either (1) reacting 1-pyrenemethoxide with a chloromethylated polystyrene backbone to yield the GrE−PS series, (2) copolymerizing styrene with 4-(1-pyrenyl)methoxymethylstyrene to yield the CoE−PS series, (3) copolymerizing styrene with *N*-(1-pyrenylmethyl)acrylamide to yield the CoA−PS series, or (4) polymerizing α,ω-dicarboxyl end-capped polystyrenes with L-lysine-1-pyrenemethylamide dihydrochloride to yield the ES−PS series. Steady-state and time-resolved fluorescence experiments demonstrated that the long and flexible linker of GrE−PS and CoE−PS enabled more efficient excimer formation than the short and rigid linker of CoA−PS, and that spacing the pyrene pendants in ES−PS led to a strong reduction in excimer formation. The fluorescence blob model (FBM) was applied to analyze quantitatively the monomer and excimer fluorescence decays of the four Py−PSs. The FBM analysis confirmed that the longer ether linker of GrE−PS and CoE−PS enabled the excited pyrene label to probe a larger volume inside the polymer coil. The level of clustering of the pyrene pendants was found to be minimal for ES−PS, as expected from its structural design. Interestingly, the pyrene pendants were twice more clustered for GrE−PS than for CoE−PS, despite both polymers having an identical chemical structure. The results for the GrE−PS and CoE−PS series suggest that reacting groups distribute themselves differently in a copolymer whether they are incorporated by a grafting onto reaction or copolymerization.

Introduction

Ever since Cuniberti and Perico[1,2] and Winnik[3] demonstrated 30 years ago that information on end-to-end chain cyclization could be obtained by labeling both ends of a chain with a pyrene moiety and monitoring excimer formation from the diffusive encounters between the two pyrene moieties, the process of pyrene excimer formation has been used to gain information about polymer chain dynamics. Since then, the use of fluorescence to monitor the encounters between two pyrene chromophores attached onto a polymer has yielded a wealth of information on long range dynamics,[4,5] conformation,[6−8] and aggregation[9,10] of polymers in solution. These fluorescence experiments are conducted by exciting a pyrene moiety with UV light and following its emission at around 375 nm. An encounter between an excited pyrene and a ground-state pyrene results in the formation of an excimer whose emission is red-shifted with respect to that of the monomer, to about 480 nm.[11] Since the pyrene moieties are attached onto the polymer, excimer formation indicates that two units of the polymer have encountered. By analyzing the process of excimer formation, information on the behavior of the polymer in solution is retrieved.[1,5]

In the majority of cases, the rule of thumb for incorporating pyrene into a polymer depends to a large extent on the labeling strategy being as easy as possible and the linker connecting pyrene to the polymer being as stable as possible in the given solvent. Once labeled, the behavior of the polymer is investigated by following the kinetics of excimer formation.[1−10] Of the numerous studies conducted using pyrene-labeled polymers, only a few have noted a difference in excimer formation when changes are made to the method of pyrene incorporation,[12] or to the length[13] or type[14] of the linker used to connect the pyrene probe to the polymer backbone. In view of the large body of studies where pyrene-labeled polymers are used,[4,5,9,10] there is a glaring lack of knowledge on the effect that the mode of pyrene incorporation into a polymer has on the very excimer formation used to draw conclusions on the polymer behavior. This study addresses this issue by investigating the effect that the three following parameters have on the process of excimer formation between pyrenes attached along a polymer chain: (1) the method of pyrene incorporation, (2) the nature of the linker connecting pyrene to the backbone, and (3) the pyrene distribution along the polymer backbone. The study focuses on pyrene-labeled polymers where pyrene is incorporated along the backbone since the preparation of such polymers is usually much less demanding[5,9,10,15−17] than that of polymers where pyrene is introduced at specific positions, typically the chain ends.[1−4]

To determine the effect of the method of pyrene incorporation, two series of pyrene labeled polystyrene (Py−PS) with identical structure were synthesized in two different ways. The first was prepared by synthesizing PS, chloromethylating a small portion of the aromatic rings, and subsequently reacting the chloromethylated backbone with 1-pyrenemethoxide. This process yields PS where pyrene was grafted onto the PS backbone via an ether linkage (GrE−PS).[18] The second was prepared by synthesizing a 4-(1-pyrenyl)methoxymethylstyrene monomer and copolymerizing it with styrene (CoE−PS). Both of these syntheses produce PS samples randomly labeled with pyrene groups which have identical chemical structure, but potentially different distributions of pyrene pendants along the chain.

To determine the effect that the linker connecting pyrene to the backbone has on excimer formation, a second copolymer was prepared using *N*-(1-pyrenylmethyl)acrylamide as the

* To whom correspondence should be addressed.

10.1021/ma070368h CCC: $37.00
Published on Web 08/09/2007

Scheme 1. Chemical Structures of CoA−PS, CoE−PS, GrE−PS, and ES−PS

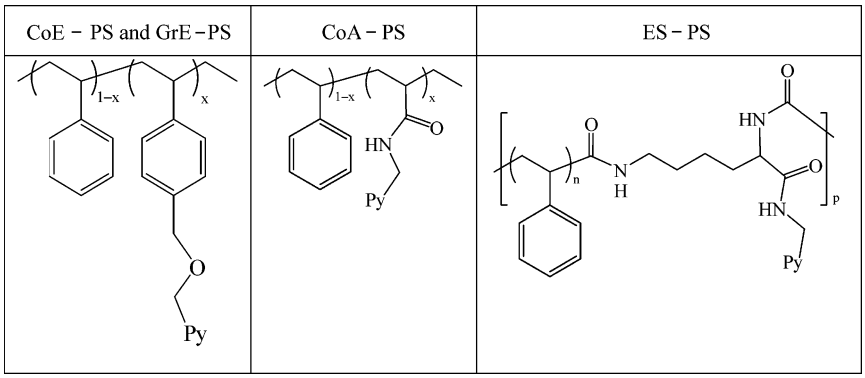

pyrenyl monomer (CoA−PS). CoE−PS and CoA−PS are expected to display a similar distribution of pyrene pendants along the backbone with the stiffer amide linker of CoA−PS keeping the pyrene much closer to the backbone than the ether linker used for the CoE−PS series.

Finally, the effect of pyrene distribution was determined by condensation of L-lysine-1-pyrenemethylamide dihydrochloride containing two free amines with short PS chains terminated with carboxylic acid functions at both ends. This route yields PS with pyrene evenly-spaced throughout the backbone (ES−PS). The side-chain structure is the same as that of the *N*-(1-pyrenylmethyl)acrylamide used for the CoA−PS series which allows the comparison of a PS sample where pyrene has been incorporated in a well-defined manner (ES−PS) with a PS sample randomly labeled with pyrene (CoA−PS).

To the best of our knowledge, this study represents the first example where the effect of the mode of pyrene incorporation into a polymer on the kinetics of excimer formation is systematically investigated. The quantitative analysis of the fluorescence data presented in this work is enabled by the recently developed fluorescence blob model (FBM).[18] Currently, this is the only analytical tool available capable of differentiating the contributions made by the chain dynamics and local pyrene concentration which both affect the formation of excimer between pyrenes attached randomly onto a polymer.[5] The body of results generated in the study is expected to become a reference point used to compare trends obtained from the kinetics of excimer formation between pyrene pendants attached onto a polymer via different methods. It is expected to facilitate the comparison between the numerous trends resulting from the vast number of studies that have been and continue to be conducted with pyrene-labeled polymers.[4,5,9,10]

Experimental Section

Materials. Chemicals were purchased from Sigma-Aldrich (Milwaukee, WI) and used as received unless otherwise stated. Distilled in glass DMF and THF were purchased from Caledon Laboratories (Georgetown, ON) and used as received. Three α,ω-dicarboxyl end-capped polystyrenes [(i) M_n = 3000, PDI = 1.10, Func. = 1.90; (ii) M_n = 4500, PDI = 1.12, Func. = 1.95; (iii) M_n = 8000, PDI = 1.09, Func. = 1.95] were purchased from Polymer Source (Montréal, QC).

Pyrene-Labeled Polystyrene Obtained by Grafting Pyrene onto the Chain (GrE—PS). The synthesis and characterization of the GrE−PS samples has been described elsewhere.[18] Molecular weights and polydispersities can be found in Table SI.1. The chemical structure of GrE−PS and all other polymers can be found in Scheme 1.

Synthesis of *N*-(1-Pyrenylmethyl)acrylamide. The synthesis and purification of *N*-(1-pyrenylmethyl)acrylamide (PyMAAm) has been described elsewhere.[19]

Synthesis of 4-(1-Pyrenyl)methoxymethylstyrene (PyMMS). In a dry 50 mL round-bottom flask, 0.09 g (0.054 mol) of sodium hydride was added to 6 mL of DMF and stirred for 5 min at room temperature. 1-Pyrenemethanol (0.575 g, 2.48 mmol) was added and stirred for 30 min at room temperature. *p*-Chloromethylstyrene (0.343 g, 2.25 mmol) was added and the solution was heated to 60 °C and stirred for 4 h. The solution was removed from the heat and precipitated into water, followed by centrifugation to isolate the solid product. The crude product was dissolved in methylene chloride ($MeCl_2$) and washed with 1 N HCl, 5 wt % sodium carbonate solution, and water. The methylene chloride was dried with Na_2SO_4 and removed by rotary evaporation. A silica gel column using hexane and methylene chloride was used to further purify the product. The solid was then recrystallized in cyclohexane to obtain a white-yellow solid in a 41% yield. 300 MHz ^{1}H NMR ($CDCl_3$) for PyMMS: δ 4.6 (s, 2H, Ar−CH_2−O), δ 5.2 (d of d, 1H, alkene trans-H), δ 5.2 (s, 2H, Py−CH_2−O), δ 5.7 (d of d, 1H, alkene cis-H), δ 6.7 (q, 1H, alkene gem-H), δ 7.4 (m, 4H, ArH), δ 7.9−8.4 (several peaks, 9H, pyrenyl H's).

Random Copolymerization. The copolymers were prepared by radical polymerization of styrene and PyMAAm or PyMMS. Styrene was purified by three successive washes with 4 M NaOH followed by two distillations under reduced pressure. The pyrene content was varied by adding increasing amounts of the pyrenyl monomer. The final pyrene content was determined postsynthesis using UV−vis analysis.

The general synthesis using PyMAAm as an example is described in detail. A Schlenk tube was flame-dried and purged with N_2, followed by the addition of 0.4 g (3.84 mmol) of styrene, 0.09 g (0.31 mmol) of PyMAAm, and 2 mL of 0.2 mg/mL AIBN in DMF. The solution was deaerated by bubbling N_2 for 15 min. The reaction was conducted at 65 °C to a conversion of approximately 0.2 to minimize composition drift. Conversion was determined through ^{1}H NMR (vide infra). The polymer was precipitated in methanol, redissolved in THF and precipitated in methanol 5−7 times to remove unreacted pyrenyl monomer. The final yield was approximately 10% in each case.

300 MHz ^{1}H NMR ($CDCl_3$) for poly(styrene-*co*-PyMMS): δ 1.2 (broad, ∼ 2H, CH_2), δ 1.8 (broad, ∼1H, CH), δ 4.5 (broad, seen in polymers with pyrene contents >5 mol %, Ar−CH_2−O), δ 5.4 (broad, seen in polymers with pyrene contents >5 mol %, Py−CH_2−O), δ 5.7, δ 6.5 and δ 7.0 (broad, 4H, ArH), δ 7.9−8.4 (broad, pyrenyl H's). UV−vis (THF): peaks at 314, 328, 344 nm.

300 MHz ^{1}H NMR ($CDCl_3$) for poly(styrene-*co*-PyMAAm): δ 1.2 (broad, ∼ 2H, CH_2), δ 1.8 (broad, ∼1H, CH), δ 5.2 (broad, seen in polymers with pyrene contents >5 mol %, Py−CH_2), δ 6.5 and δ 7.0 (broad, 4H, ArH), δ 7.9−8.4 (broad, pyrenyl H's). UV−vis (THF): peaks at 314, 328, 344 nm.

Molecular Weight Determination. Apparent molecular weights were determined by gel permeation chromatography (GPC) with a Waters system using THF as an eluent and a Jordi linear DVB mixed-bed column. The instrument was coupled with a DRI detector. The column was calibrated using known molecular weight polystyrene standards. These experiments were carried out at room

temperature. Many of the M_n values were in the ~30 K range with a polydispersity index (PDI) around 1.8−2.0 (Table SI.1 in the Supporting Information).

An earlier study on pyrene-labeled GrE−PS demonstrated that the fluorescence signal of the randomly labeled polymers does not depend on polymer chain length as long as the polymer chain length is longer than a *critical polymer chain length* (*cpcl*) whose value was estimated to lay between 6 and 40 K.[18] Consequently, a 30 K PS sample with a PDI of 2.0 might contain a substantial fraction of chains whose chain length is smaller than the *cpcl*. As a result, GPC was used to fractionate the PS samples. The fluorescence experiments were run with the whole Py−PS samples, as well as their fractions containing a polymer molecular weight larger than 40 K (Table SI.2). Within experimental error, no discrepancy could be found between the results whether the fluorescence experiments were conducted with the whole Py−PS sample or the Py−PS fraction having a larger molecular weight. (See Figures SI.1 and SI.2 and Tables SI.3−SI.10 in the Supporting Information). Nevertheless, the Results and Discussion sections present the results obtained from the steady-state and time-resolved fluorescence experiments conducted on the high molecular weight fractions to ensure that all conclusions are drawn from data acquired with polymers whose chain length is larger than the *cpcl*.

Composition Drift During Polymerization. The reactivity ratios for styrene and *p*-chloromethylstyrene in benzene are 0.62 and 1.12, respectively.[20] The reactivity ratios for styrene and *N*-methylacrylamide in dioxane are 2.10 and 0.64, respectively.[21] The different reactivity ratios imply that some composition drift might occur during the copolymerization. To minimize this eventuality, the copolymerizations were conducted up to a low conversion. Changes in monomer incorporation into the copolymer were monitored as a function of conversion for both copolymerizations. Samples were removed periodically during the reaction. ^{1}H NMR was used to determine the conversion and GPC coupled with a fluorescence detector was employed to determine the ratio of the fluorescence intensity of the excimer over that of the monomer, the I_E/I_M ratio, as a function of conversion to detect eventual deviations from a random incorporation of the pyrene labeled monomers. The I_E/I_M ratio is sensitive to the pyrene content of the polymer and is expected to respond to an eventual composition drift during the copolymerization.

The conversion of the reaction was determined by integrating the vinyl monomer peaks in the ^{1}H NMR spectrum relative to the signal of trifluoroacetic acid (TFA) which was placed in a small insert at the center of the NMR tube containing a measured aliquot of the reaction solution in $CDCl_3$. For the copolymerization between styrene and PyMAAm, the monomer peaks used were located at 5.7 and 6.1 ppm, respectively. For the copolymerization of styrene and PyMMS, the peaks overlapped at 5.7 ppm and were integrated together. The same insert was used for the acquisition of each NMR spectrum and the signal of the TFA standard was taken as a reference. Thus, as the monomers were consumed, the vinyl peaks at 5.7 and 6.1 ppm decreased, and the monomer conversion was calculated. The samples were also injected into a GPC equipped with an online Agilent 1100 series fluorescence detector. The GPC column enabled the separation of the labeled polymer from the unreacted pyrene-labeled monomer. The I_E/I_M ratios were obtained for the peak corresponding to the polymer in the GPC trace (I_E = 490 nm; I_M = 390 nm). Within experimental error, the I_E/I_M ratios remained constant over the low conversion (~0.2) used for these copolymerizations. Two examples are shown in Table SI.11 in the Supporting Information.

Synthesis of L-Lysine-1-pyrenemethylamide Dihydrochloride. Into a round-bottom flask were added 0.5 g (1.07 mmol) of N_α,N_ϵ-di-Boc-L-lysine paranitrophenol ester (Bachem Chemicals), 0.258 g (0.963 mmol) of 1-pyrenemethylamine hydrochloride, 0.2 g (1.98 mmol) of triethylamine, and 20 mL of $MeCl_2$. The reaction was stirred overnight at room temperature. The reaction mixture was extracted with 2 × 1 M HCl, 2 × 5 wt % sodium bicarbonate solution, and 2 × water. The $MeCl_2$ solution was dried over $MgSO_4$, filtered, and the $MeCl_2$ was removed by rotary evaporation. The remaining solid was washed in a 1:1 benzene:hexane mixture and N_α,N_ϵ-di-Boc-L-lysine-1-pyrenemethylamide was recovered in an 85% yield.

300 MHz ^{1}H NMR (DMSO-d_6) for N_α,N_ϵ-di-Boc-L-lysine-1-pyrenemethylamide: δ 1.3 (broad, 18H *t*-boc and 4H, 2 × CH_2), δ 1.5 (m, 2H, CH_2), δ 2.8 (m, 2H, CH_2), δ 3.9 (broad, 1H, CH), δ 5.0 (m, 2H, Py-CH_2), δ 6.7 (t, 1H, NH), δ 6.9 (d, 1H, NH), δ 7.9−8.4 (many sharp pyrene peaks, broad amine peaks), δ 8.5 (t, 1H, amide NH).

Into a round-bottom flask were added 0.4 g (0.714 mmol) of N_α,N_ϵ-di-Boc-L-lysine-1-pyrenemethylamide and 10 mL of 4 M HCl in dioxane. The mixture was stirred for 1 h. Dioxane was removed by rotary evaporation, and the L-lysine-1-pyrenemethylamide dihydrochloride was precipitated as a solid product in ether in a 90% yield.

300 MHz ^{1}H NMR (DMSO-d_6) L-lysine-1-pyrenemethylamide dihydrochloride: δ 1.3 (m, 2H CH_2), δ 1.4 (m, 2H, CH_2), δ 1.7 (m, 2H, CH_2), δ 2.6 (m, 2H, CH_2), δ 3.8 (m, 1H, CH), δ 5.1 (d, 2H, Py-CH_2), δ 7.9−8.4 (many sharp pyrene peaks, broad amine peaks), δ 9.3 (t, 1H, amide NH).

Synthesis of Evenly-Spaced Polystyrene (ES−PS). The ES−PS samples were prepared by copolymerizing α,ω-dicarboxyl end-capped polystyrene having M_n equal to 3000, 4500, and 8000 g/mol with L-lysine-1-pyrenemethylamide dihydrochloride. An example synthesis is described for the polymer having an M_n of 4500 g/mol.

Into a 7 mL vial were added 0.1 g (0.0222 mmol) of 4500 g/mol α,ω-dicarboxyl end-capped polystyrene, 0.0096 g (0.222 mmol) of L-lysine-1-pyrenemethylamide dihydrochloride, 0.042 g (0.222 mmol) of EDC, 0.030 g (0.222 mmol) of HOBt, 0.50 g (0.05 mmol) of triethylamine, and 1 mL of DMF. The reaction was stirred at room temperature for 20 h. The polymer was precipitated in methanol, redissolved in THF, and precipitated in methanol 5−7 times to remove unreacted pyrenyl monomer. A very broad molecular weight distribution was obtained. The ES−PS sample contained a substantial amount of the PS starting material which could not be separated from the longer polymer chains using precipitation. To circumvent this problem, the polymer was fractionated using GPC to obtain a high molecular weight (HMW) fraction used for the fluorescence experiments. Molecular weights of the HMW fractions were determined using the fluorescence detector calibrated with polystyrene standards and are found in Table SI.2. Only the HMW fractions of the ES−PS samples were investigated.

Pyrene Content. A Hewlett-Packard 8452A diode array spectrophotometer was used for the absorption measurements. The copolymer composition was determined from its pyrene content.

The pyrene content of the polymer (λ) is obtained by dissolving a known mass of pyrene labeled polymer (m) in a known volume of THF (V). The concentration of pyrene, [*Py*], is then determined by applying Beer−Lambert's law to the peak absorption at 344 nm and using the extinction coefficient of the model compound 1-pyrenemethanol in THF (ϵ_{py}) found to equal 43 000 $M^{-1}cm^{-1}$. The pyrene content, λ, whose expression is given in eq 1, is expressed in micromoles of pyrene per gram of polymer (μmol g^{-1}).

$$\lambda = \frac{[\mathrm{Py}]}{m/V} \tag{1}$$

Steady-State Fluorescence Measurements. All fluorescence spectra were acquired on a PTI fluorometer. The spectra were obtained with the usual right angle geometry. Polymer solutions had a pyrene concentration below 3 × 10^{-6} M to avoid intermolecular interactions and were degassed with N_2 for 20 min to remove oxygen. The solution OD was ~ 0.1 at 344 nm in each case. The solutions were excited at 344 nm and the fluorescence intensity of the monomer (I_M) and excimer (I_E) were obtained by integrating the fluorescence intensity between 372 and 378 nm for the monomer and 500−530 nm for the excimer, respectively.

Time-Resolved Fluorescence Measurements. Monomer and excimer decays were obtained by exciting the solutions at 340 nm with an IBH 340 nm LED laser and monitoring the fluorescence emission at 375 and 510 nm, respectively. All decays were collected over 1024 channels with up to 20 000 counts at the peak maximum for the lamp and decay curves. The instrument response function was determined by applying the MIMIC method[22] to the lamp reference decays obtained with PPO [2,5-diphenyloxazole] in cyclohexanol ($\tau = 1.42$ ns) and BBOT [2,5-bis(*tert*-butyl-2-benzoxazolyl)thiopene] in ethanol ($\tau = 1.47$ ns) for the monomer and excimer decays, respectively. The polymer solutions were prepared in the same manner as for the steady-state fluorescence experiments.

Analysis of the Fluorescence Decays. The fluorescence decays of the monomer and excimer were fit with a sum of exponentials (eq 2) or by using a global analysis based on the Fluorescence Blob Model (FBM) to fit the monomer (eq 3) and excimer (eq 5) simultaneously.[23] In the FBM framework, a *blob* represents the volume probed by an excited pyrene while it remains excited. Equation 3 was originally developed by applying the same mathematical derivation used to describe the formation of excimer between pyrene molecules distributed in surfactant micelles,[24] but has since been used in several recent publications to study polymer dynamics in solution.[5,18,19,23,25,26]

$$i(t) = \sum_{i=1}^{n_{exp}} a_i \exp(-t/\tau_i) \quad \text{with} \quad n_{exp} = 2-4 \tag{2}$$

$$[\mathrm{Py}^*]_{(t)} = [\mathrm{Py}^*_{diff}]_{(t=0)} \exp\left[-\left(A_2 + \frac{1}{\tau_M}\right)t - A_3(1-\exp(-A_4 t))\right] + [\mathrm{Py}^*_{free}]_{(t=0)} \exp(-t/\tau_M) \tag{3}$$

The parameters A_2, A_3, and A_4 used in eq 3 are described in eq 4.

$$A_2 = \langle n \rangle \frac{k_{blob} k_e[\mathrm{blob}]}{k_{blob} + k_e[\mathrm{blob}]}$$

$$A_3 = \langle n \rangle \frac{{k_{blob}}^2}{(k_{blob} + k_e[\mathrm{blob}])^2}$$

$$A_4 = k_{blob} + k_e[\mathrm{blob}] \tag{4}$$

The first exponential of eq 3, which is used to fit the monomer decays, assumes that excimer formation occurs via diffusion between pyrene monomers, $[\mathrm{Py}^*_{diff}]$. In the first exponential of eq 3, three parameters are retrieved that describe the kinetics of excimer formation for a given pyrene labeled polymer. They are the rate constant for excimer formation by diffusion between one excited pyrene and one ground-state pyrene located in the same blob, k_{blob}, the average number of ground-state pyrenes per blob, $\langle n \rangle$, and the rate constant for the exchange of ground-state pyrenes between blobs times the concentration of blobs in the polymer coil, k_e[blob]. The second exponential accounts for the fluorescence of any unquenched pyrene monomer, $[\mathrm{Py}^*_{free}]$, that fluoresces with its natural lifetime, τ_M. These long-lived species do not form excimer and thus are not described by the FBM. For each Py−PS series, a low pyrene content polymer (<0.2 mol %) was synthesized. With the low pyrene content, very little excimer is formed and fitting the monomer decays with a sum of exponentials (eq 2) resulted in a strong contribution (>80%) from pyrenes emitting with their natural lifetime, τ_M. The τ_M values retrieved from this analysis were in the 253−259 ns range for all Py−PS samples in THF (Table SI.12). All analyses presented in this work were conducted with a τ_M value set to equal 260 ns.

$$[\mathrm{E}^*] = -[\mathrm{Py}^*_{diff}]_{(t=0)} e^{-A_3} \sum_{i=0}^{\infty} \frac{{A_3}^i}{i!} \frac{A_2 + iA_4}{\frac{1}{\tau_M} - \frac{1}{\tau_{E0}} + A_2 + iA_4} \exp\left(-\left(\frac{1}{\tau_M} + A_2 + iA_4\right)t\right) + \left([\mathrm{E0}^*]_{(t=0)} + [\mathrm{Py}^*_{diff}]_{(t=0)} e^{-A_3} \sum_{i=0}^{\infty} \frac{{A_3}^i}{i!} \frac{A_2 + iA_4}{\frac{1}{\tau_M} - \frac{1}{\tau_{E0}} + A_2 + iA_4}\right) e^{-t/\tau_{E0}} + [\mathrm{D}^*]_0 e^{-t/\tau_D} \tag{5}$$

The excimer decays were fit using eq 5, where τ_{E0} is the excimer lifetime. Equation 5, which was derived and applied in earlier studies,[19,26−29] assumes that the excimer is formed and emits as one of three species in solution. These species result from the diffusional encounter of an excited pyrene monomer and a ground-state pyrene, and the direct excitation of ground-state dimers (E0*) and long-lived ground-state dimers (D*). The fits of the monomer and excimer decays with eqs 3 and 5 enables one to determine the fractions of all pyrene species, Py_{diff}, Py_{free}, E0, and D, in solution. The fraction of aggregated pyrenes, f_{agg}, is the sum of $f_{E0} + f_D$. A more detailed explanation on the determination of the fractions is found in previous works.[19,26−29]

Optimization of the parameters used in eqs 2, 3, and 5 to fit the fluorescence decays was performed with the Marquardt−Levenberg algorithm.[30] The IBH 340 LED laser used to acquire the fluorescence decays was found to generate a higher noise level than the IBH hydrogen lamp used previously.[23,28] Consequently, a background correction was applied to fit the fluorescence decays.[31] As was done in earlier publications, a light scattering correction was also applied to account for those pyrene pairs which are in close contact and form excimer on a time scale which is too fast to be detected accurately by our instrument.[31] The fits of the monomer and excimer decays were considered good if the χ^2 was below 1.4 and the residuals were randomly distributed around zero (see Figures SI.3 and SI.4 for sample decays).

Results

The steady-state fluorescence spectra were obtained in THF for all polystyrene samples. The spectra of the Py−PS samples containing ~3.5 mol % pyrene are shown in Figure 1. The largest amount of excimer is obtained with the GrE−PS and CoE−PS samples. The ES−PS sample forms the least excimer, and the CoA−PS sample generates an intermediate amount of excimer. Qualitatively, this result demonstrates that the process of excimer formation depends strongly on the method of pyrene incorporation. The ratios of the fluorescence intensity of the monomer over that of the excimer, the I_E/I_M ratios, are plotted as a function of pyrene content for the four Py−PS series in Figure 2. For each series, I_E/I_M increases exponentially with pyrene content, as found in previous studies of polymers randomly labeled with pyrene.[18,19,26] The same differences in excimer formation observed for the samples containing ~3.5 mol % of pyrene in Figure 1 are found over the entire range of pyrene contents. The series with major structural differences (side-chain type and pyrene distribution) generate very different amounts of excimer over the entire range of pyrene contents, while the two series with identical chemical structures, namely CoE−PS and GrE−PS, follow a similar trend.

The monomer and excimer decays were acquired and analyzed using a multiexponential fit usually resulting in χ^2 smaller than 1.3. The decay times and pre-exponential factors are reported in Tables SI.3 and SI.4 in the Supporting Information. The monomer decays were analyzed using up to four

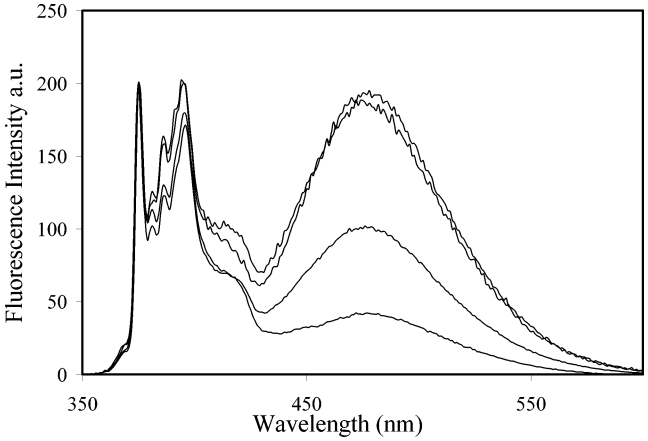

Figure 1. Steady-state fluorescence spectra of polystyrene labeled with ~3.5 mol % pyrene in THF. From top to bottom: CoE−PS, GrE−PS, CoA−PS, and ES−PS. [Py] = 3×10^{-6} M; λ_{ex} = 344 nm.

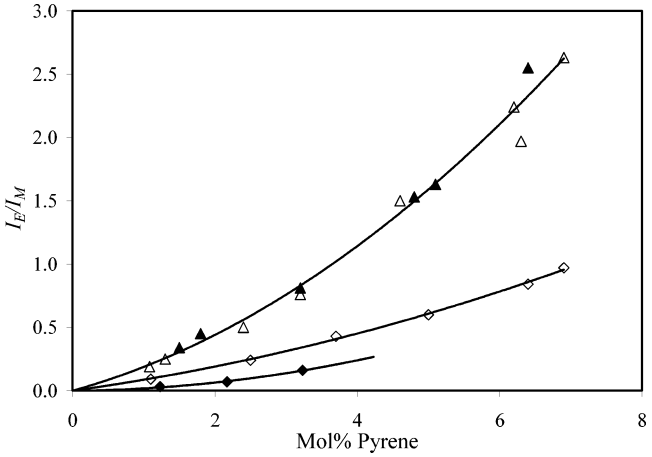

Figure 2. I_E/I_M ratios as a function of pyrene content: GrE−PS (△), CoE−PS (▲), CoA−PS (◇), and ES−PS (◆). [Py] = 3×10^{-6} M; λ_{ex} = 344 nm. Error analysis on some of the I_E/I_M ratios is provided in Table SI.14.

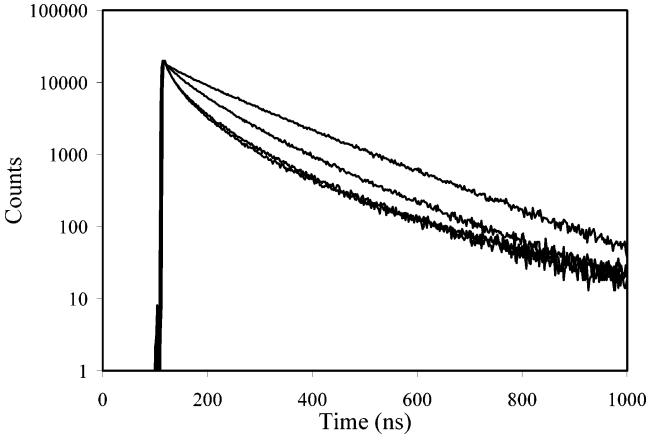

Figure 3. Monomer fluorescence decays of polystyrene labeled with ~3.5 mol % pyrene in THF. From top to bottom: ES−PS, CoA−PS, CoE−PS, and GrE−PS. [Py] = 3×10^{-6} M, λ_{ex} = 340 nm, and λ_{em} = 375 nm.

exponentials with the longest decay time fixed to τ_M, the lifetime of the pyrene label in THF (260 ns). The fluorescence decays of the pyrene monomer for the Py−PS samples containing ~3.5 mol % of pyrene are shown in Figure 3. The pyrene monomer decays more quickly according to the sequence ES−PS < CoA−PS < CoE−PS ≅ GrE−PS. Since a steeper monomer decay reflects an increased excimer production, the trend

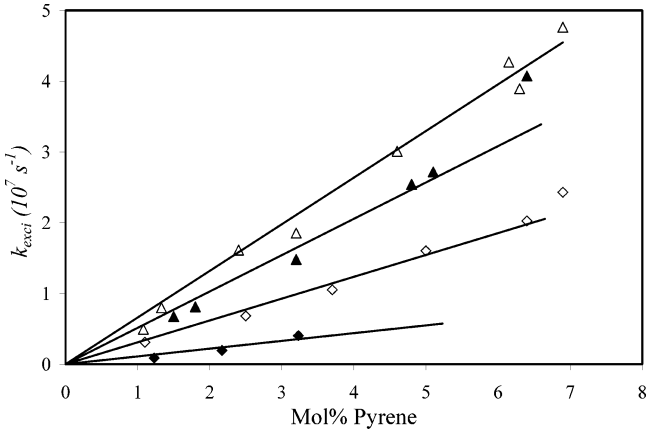

Figure 4. k_{exci} as a function of pyrene content: GrE−PS (△), CoE−PS (▲), CoA−PS (◇), and ES−PS (◆). [Py] = 3×10^{-6} M. Error analysis on some of the k_{exci} values is provided in Table SI.15

obtained in Figure 3 by time-resolved fluorescence is similar to that obtained in Figure 1 by steady-state fluorescence. The results obtained from the analysis of the monomer decays with a sum of exponentials can be used to estimate the pseudo-unimolecular rate constant of excimer formation, k_{exci}, according to eq 6 which has been applied earlier.[32]

$$k_{exci} = \frac{1}{\langle \tau \rangle} - \frac{1}{\tau_M} \tag{6}$$

In eq 6, $\langle \tau \rangle$ represents the number-average decay time of the pyrene monomer, while τ_M represents the unquenched lifetime of the monomer. Figure 4 gives the trends obtained by plotting k_{exci} as a function of the pyrene content of the four PS samples. According to eq 6, a larger k_{exci} implies a more efficient excimer formation. The trends shown in Figure 4 indicate that the efficiency of excimer formation increases according to the sequence: ES−PS < CoA−PS < CoE−PS ≤ GrE−PS. The rate of excimer formation can usually be compared to the I_E/I_M ratio since a larger k_{exci} results in a larger I_E/I_M ratio. The I_E/I_M ratios and k_{exci} values shown in Figures 2 and 4 for ES−PS, CoA−PS, and CoE−PS yield the expected trends. However, although the I_E/I_M ratios of CoE−PS and GrE−PS yield identical trends in Figure 2, k_{exci} of GrE−PS appears to be substantially larger than k_{exci} of CoE−PS in Figure 4. Since the chemical structures of GrE−PS and CoE−PS are identical, an increase of the rate of excimer formation suggests that the pyrene pendants are incorporated closer to one another in GrE−PS.

An indication that this might be the case is obtained from the close inspection of the P_A and a_{E-}/a_{E+} ratios. The peak-to-valley ratio or P_A ratio has been shown to take a lower value than 3.0 when pyrene aggregates are present in solution.[9] Similarly, the a_{E-}/a_{E+} ratio obtained from the ratio of the sum of the negative pre-exponential factors of the excimer decay over the sum of the positive ones takes values more positive than −1.0 in the presence of pyrene aggregates.[19,27] The P_A values for GrE−PS and CoE−PS were 2.83 ± 0.06 and 3.02 ± 0.03, respectively, while the a_{E-}/a_{E+} ratios were −0.74 ± 0.04 and −0.85 ± 0.04, respectively. Both ratios indicate that the GrE−PS series bears pyrene pendants which are more aggregated than in the CoE−PS series. The clustering of the pyrene pendants implies that some pyrenes are attached on neighboring styrene units. This geometric arrangement restricts the number of conformations available to two pyrene neighbors preventing them from adopting the ideal stacking required for excimer formation. As a result, excimers formed by clustered

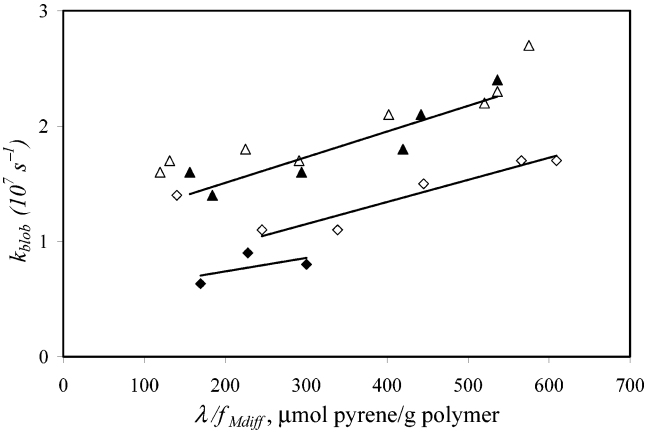

Figure 5. k_{blob} as a function of pyrene content: GrE−PS (△), CoE−PS (▲), CoA−PS (◇), and ES−PS (◆). [Py] = 3 × 10^{-6} M.

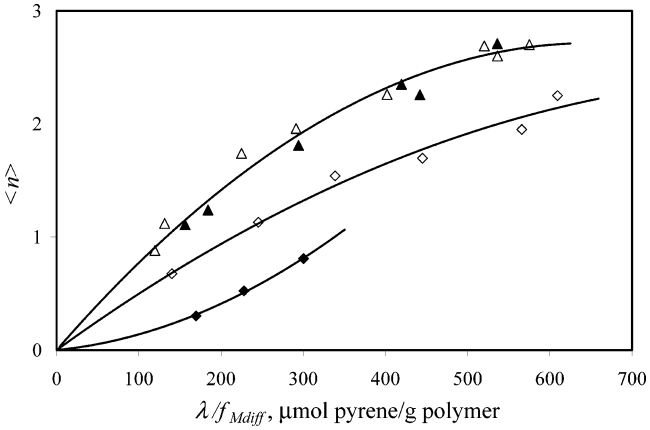

Figure 6. ⟨*n*⟩ as a function of pyrene content: GrE−PS (△), CoE−PS (▲), CoA−PS (◇), and ES−PS (◆). [Py] = 3 × 10^{-6} M.

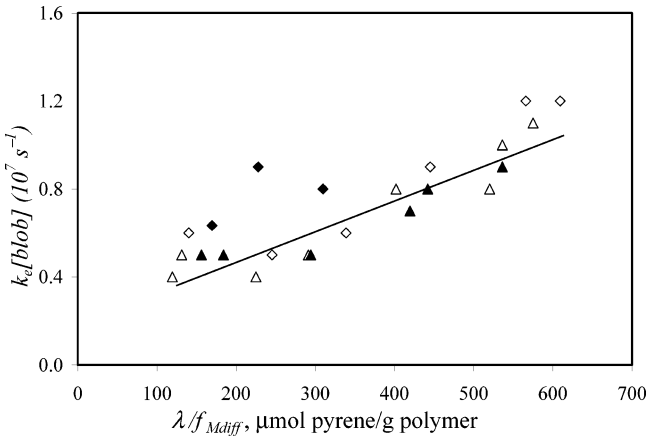

Figure 7. k_e[blob] as a function of pyrene content: GrE−PS (△), CoE−PS (▲), CoA−PS (◇), and ES−PS (◆). [Py] = 3 × 10^{-6} M.

pyrenes have a lower quantum yield than excimers formed from the diffusive encounter between two pyrenes.[13,33−35]

The influence of aggregation is most likely the reason for the discrepancy between the steady-state (Figure 2) and time-resolved (Figure 4) fluorescence data. The clustering of the pyrenes leads to faster excimer formation since the pyrene pendants are close to one another, but also a lower excimer fluorescence emission due to poor stacking.[13,33−35] The two effects seem to cancel each other out resulting in a similar trend for the I_E/I_M ratios obtained for CoE−PS and GrE−PS in Figure 2. This example highlights the need for caution when determining rates of excimer formation qualitatively using I_E/I_M ratios alone.

Although pronounced differences are observed in the process of excimer formation depending on the method of incorporation of pyrene into the polymer, little can be inferred about the reasons causing the differences observed by steady-state (Figures 1 and 2) and time-resolved (Figures 3 and 4) fluorescence. A more comprehensive picture about the process of excimer formation can only be achieved through the quantitative analysis of the pyrene monomer and excimer fluorescence decays of the pyrene labeled polymers using the fluorescence blob model (FBM).[5]

FBM Results. Over the last number of years, numerous polymers randomly labeled with pyrene have been studied with an analysis based on the FBM.[5,18,19,25−29] Equations 3 and 5 are used to fit the monomer and excimer decays, respectively, to retrieve the parameters k_{blob}, k_e[blob], and ⟨*n*⟩. These parameters were obtained from fitting the decays acquired with all Py−PS samples. They are listed in Tables SI.5−10 in the Supporting Information. Plots of k_{blob}, ⟨*n*⟩, and k_e[blob] as a function of pyrene content are found in Figures 5−7. The corrected pyrene content, λ/f_{Mdiff}, is introduced in Figures 5−7 to account for those domains of the polymer that are pyrene poor and do not form any excimer. The fraction f_{Mdiff} is equal to $[Py^*_{diff}]_{(t=0)}/([Py^*_{diff}]_{(t=0)} + [Py^*_{free}]_{(t=0)})$ and is obtained from eq 3. It is usually close to 1.0 for pyrene contents greater than 2.5 mol % so that this correction is not too important. For all Py−PS series, k_{blob} increases gently with pyrene content, k_e[blob] exhibits a slightly more pronounced increase with increasing pyrene content, and ⟨*n*⟩ increases with increasing pyrene content over the range studied. The trends shown in Figures 5−7 are consistent with those obtained with a series of pyrene-labeled poly(*N*,*N*-dimethylacrylamides) (Py−PDMA) in acetone and DMF.[19]

Extensive studies have been completed on Py−PDMA using the FBM.[19,25] One of the important conclusions drawn from these studies was that k_{blob} is a pseudo-unimolecular rate constant that is the product of the rate constant for diffusive encounter between an excited pyrene and a ground-state pyrene, k_{diff}, and the inverse of the blob volume, $1/V_{blob}$ (eq 7).[19,25] eq 7 implies that multiplying k_{blob} by ⟨*n*⟩ yields a measure of the *local pyrene concentration*, $[Py]_{loc}$, equal to $\langle n\rangle/V_{blob}$. A plot of $k_{blob} \times \langle n\rangle$ vs pyrene content is shown in Figure 8. As expected, a linear increase in $k_{blob} \times \langle n\rangle$ is observed with increasing pyrene content for all four polymer series, reflecting the linear dependence of $[Py]_{loc}$ with pyrene content.

$$k_{blob} = k_{diff} \times \frac{1}{V_{blob}} \tag{7}$$

The $k_{blob} \times \langle n\rangle$ values shown in Figure 8 suggest that $[Py]_{loc}$ increases according to the sequence ES−PS < CoA−PS < CoE−PS < GrE−PS. Since excimer formation depends on $[Py]_{loc}$, k_{exci} should also be a measure of $[Py]_{loc}$. The $k_{blob} \times \langle n\rangle$ trends obtained in Figure 8 are in agreement with the k_{exci} trends shown in Figure 4. At a given pyrene content, the k_{exci} values for GrE−PS are 1.3 ± 0.1 times larger than those for CoE−PS, which are themselves 1.6 ± 0.2 times larger than those obtained for CoA−PS, themselves 2.8 ± 0.7 times larger than for ES−PS. Similarly, the $k_{blob} \times \langle n\rangle$ products at a given pyrene content reported in Figure 8 for GrE−PS are 1.2 ± 0.2 times larger than those for CoE−PS, which are themselves 1.8 ± 0.2

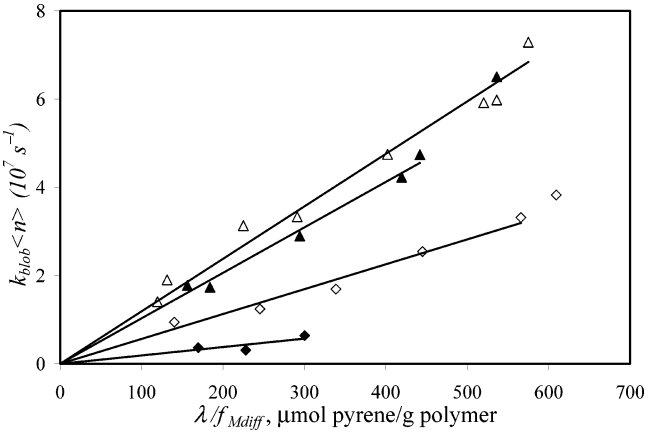

Figure 8. $k_{blob} \times \langle n \rangle$ as a function of pyrene content: GrE−PS (△), CoE−PS (▲), CoA−PS (◇), and ES−PS (◆). [Py] = 3×10^{-6} M.

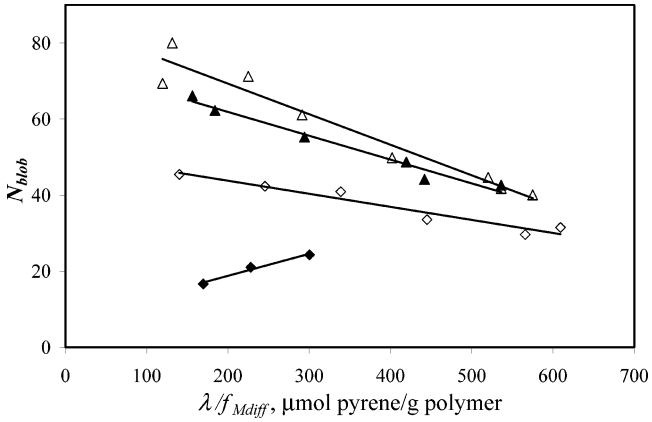

Figure 9. N_{blob} as a function of pyrene content: GrE−PS (△), CoE−PS (▲), CoA−PS (◇), and ES−PS (◆). [Py] = 3×10^{-6} M.

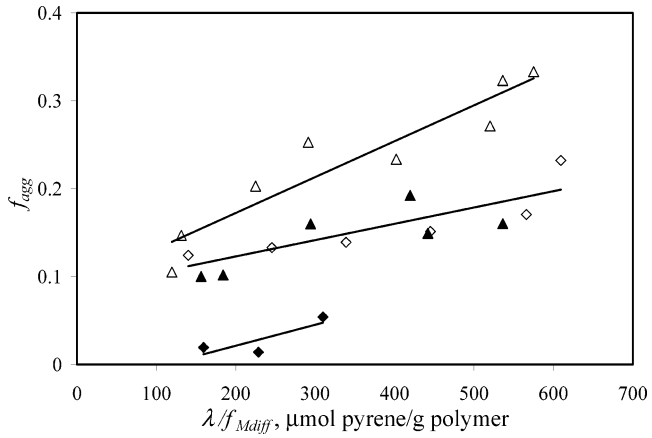

Figure 10. f_{agg} as a function of pyrene content: GrE−PS (△), CoE−PS (▲), CoA−PS (△), and ES−PS (◆). [Py] = 3×10^{-6} M.

times larger than those obtained for CoA−PS, themselves being 2.9 ± 0.6 times larger than for ES−PS. The actual slopes and errors on the slope of the trends shown in Figures 4 and 8 can be found in Table SI.13. The agreement obtained between the trends of k_{exci} and $k_{blob} \times \langle n \rangle$ vs pyrene content further supports the assertion made earlier[19,25] that the product $k_{blob} \times \langle n \rangle$ is a measure of $[Py]_{loc}$.

If the product $k_{blob} \times \langle n \rangle$ is a measure of $[Py]_{loc}$, one might ask why all $k_{blob} \times \langle n \rangle$ values do not merge on a single master curve in Figure 8. The reason why this is not the case lays in the excimer formation depending not only on $[Py]_{loc}$, but also on the flexibility of the chain and linker connecting the pyrene probe to the chain. As will be discussed later on, faster chain and linker dynamics result in more efficient excimer formation for polymers having a same $[Py]_{loc}$. The inherent ability of the FBM to differentiate between the contributions to excimer formation due to polymer chain dynamics and $[Py]_{loc}$ by using, respectively, k_{blob} and $\langle n \rangle$ is what constitute the main advantage of the FBM over more traditional analyses of excimer formation with pyrene-labeled polymers that rely only on the I_E/I_M ratio and k_{exci}.

Besides k_{blob} which is inversely proportional to V_{blob} (eq 7), a second general measure of the volume probed by an excited pyrene, V_{blob}, is obtained from N_{blob}, which is the number of styrene monomers constituting a blob.[5] N_{blob} is calculated with eq 8, where $\langle n \rangle$ is the average number of pyrenes per blob, retrieved from the FBM analysis of the monomer decays, M_{Py} is the molecular weight of the pyrene labeled monomer, M_{Sty} is the molecular weight of the styrene monomer, x is the mole fraction of the pyrene labeled monomer, λ is the pyrene content in moles of pyrene per gram of polymer, and f_{Mdiff} is the fraction of pyrenes that form excimer by diffusion.

$$N_{blob} = \frac{\langle n \rangle}{\lambda / f_{Mdiff}[M_{Py}(x) + M_{Sty}(1-x)]} \qquad (8)$$

Regardless of pyrene content, N_{blob} is found to increase according to the sequence ES−PS < CoA−PS < CoE−PS ≅ GrE−PS (Figure 9). For each PS series except that of ES−PS, N_{blob} increases with decreasing pyrene content. The value of N_{blob} for a pyrene labeled polymer is found by extrapolating the trends shown in Figure 9 to zero pyrene content, where potential distortions of the polymer conformation induced by the pyrene labels are expected to be minimized.[18,26] N_{blob} was found to equal 85 ± 4, 74 ± 4, 51 ± 3, and 20 ± 3 styrene units for GrE−PS, CoE−PS, CoA−PS, and ES−PS, respectively. Since a *blob* is the volume probed by an excited pyrene, the differences in N_{blob} shown in Figure 9 imply that the mode of pyrene incorporation into a polymer does affect its mobility.

Comparison of the N_{blob} values for the CoA−PS and CoE−PS series indicates that V_{blob} increases with increasing length of the linker connecting pyrene to the backbone. Yet, eq 7 predicts that this increase in V_{blob} should be accompanied by a decrease in k_{blob}. Interestingly, the opposite is observed in Figure 5. The parallel increase of k_{blob} and V_{blob} with increasing linker length implies that k_{diff} in eq 7 must increase substantially to offset the change in V_{blob}. This interesting development is probed in more detail in the Discussion section.

The FBM parameters account for those pyrenes that form excimer by diffusion. However, an excimer can also be produced by the direct excitation of a pyrene cluster.[9] As discussed earlier, pyrene aggregation affects excimer formation and thus, the I_E/I_M ratios in Figure 2. The fraction of aggregated pyrene pendants, f_{agg}, is retrieved from the analysis of the monomer and excimer fluorescence decays and has been used extensively to study the associative strength of associative polymers (AP) where the associating moiety is either pyrene or labeled with pyrene.[19,23,26−29]

The plot of f_{agg} vs pyrene content in Figure 10 indicates that the pyrenyl pendants are much less aggregated in the ES−PS series than in any of the other Py−PSs. This is reasonable since the synthetic route followed to generate the ES−PS series forces the pyrenes apart along the backbone preventing them from being located adjacent to one another. The other three Py−PSs,

however, show a quite remarkable result. The two polymers obtained by copolymerizing styrene with a pyrene labeled monomer (CoA−PS and CoE−PS) have a similar level of aggregation, but the GrE−PS series yields a significantly higher f_{agg} at almost all pyrene contents. This result suggests that the pyrene groups are **not** incorporated in the same manner depending on the synthetic method being used.

Discussion

(1) Effect of the Method of Pyrene Incorporation. The CoE−PS and GrE−PS series were synthesized to determine whether the synthetic route taken to build a pyrene labeled polymer would play any role in the formation of excimers. These two series should both produce randomly labeled copolymers with identical chemical composition, and thus should form excimer in a similar manner. However, it was found that although their I_E/I_M ratios were similar, the k_{exci} and f_{agg} values shown in Figures 4 and 10 indicate that the pyrenyl pendants are more clustered in GrE−PS than in CoE−PS.

The higher level of aggregation is also reflected in the slightly increased local pyrene concentration in the GrE−PS series given by $k_{blob} \times \langle n \rangle$ as seen in Figure 8. The larger f_{agg} values and higher $[Py]_{loc}$ obtained for GrE−PS might also explain why, although the N_{blob} vs pyrene content (λ/f_{Mdiff}) trends shown in Figure 9 are similar for GrE−PS and CoE−PS, extrapolating the trends to $\lambda/f_{Mdiff} = 0$ yields a slightly lower N_{blob} value for CoE−PS (74 ± 4) than for GrE−PS (85 ± 4). Indeed, a higher $[Py]_{loc}$ results in a higher $\langle n \rangle$ value, which according to eq 8, yields a larger N_{blob} value.

The higher clustering of the pyrene pendants observed with GrE−PS could be caused by two different effects, or a combination of both. The first possibility is that the graft-onto modification reaction occurs in a clustered manner. Since a polymer coil is expected to be denser at its center according to Flory,[36] the chloromethylation reaction used in the preparation of GrE−PS[18] could be favored toward the center of the polymer coils, resulting in an increased local pyrene concentration toward the center of the polymer coil and thus an increased clustering of the pyrene groups in GrE−PS. Copolymerization, which depends only on the reactive end of the growing chain, ensures that the pyrene labeled comonomers are incorporated throughout the chain, minimizing the probability of forming pyrene clusters. The second reason for observing an increased level of pyrene clustering in the GrE−PS series could be an undesired side effect of the polymer modification. The chloromethylation reaction is known to induce cross-linking.[37] Precautions were taken to prevent cross-linking during the chloromethylation reaction by using relatively low polymer concentrations, and no evidence of intermolecular cross-linking was found in the GPC traces of the chloromethylated polystyrenes.[18] Nevertheless, the occurrence of intramolecular cross-linking cannot be ignored. Since its effect on excimer formation of a pyrene labeled polymer has not been previously explored, it remains a possible explanation for the discrepancy. In any case, the data obtained by time-resolved fluorescence demonstrate that the two synthetic methods used to prepare CoE−PS and GrE−PS yield similar polymers but with different levels of clustering of the pyrene pendants that affect excimer formation.

(2) Effect of Linker Length on Excimer Formation. The copolymers CoE−PS and CoA−PS were prepared to assess the effect that the length of the linker connecting the pyrene probe to the PS backbone has on excimer formation. The main differences for the two copolymer series are observed for the parameters k_{blob} (Figure 5), $\langle n \rangle$ (Figure 6), and N_{blob} (Figure 9). The value of each of these parameters is always smaller for the CoA−PS series than for the CoE−PS series. These differences are certainly due to the longer reach and the increased flexibility enabled by the ether linker of the CoE−PS series (Scheme 1).

According to the definition of a *blob*, N_{blob} represents the number of monomer units constituting a *blob*. Since N_{blob} for CoE−PS (74 ± 4) is larger than for CoA−PS (51 ± 3), V_{blob} for CoE−PS must be larger than that for CoA−PS. An estimate of V_{blob} can be obtained by using the Mark−Houwink−Sakurada equation to determine the hydrodynamic volume V_h of a PS chain made of N_{blob} units. Using the $K = 0.011$ mL/g and $a = 0.725$ values for PS in THF,[38] one finds that the hydrodynamic radius of a *blob*, R_h, equals 1.7 and 2.1 nm for CoA−PS and CoE−PS, respectively. The increase in R_h results in a 1.9 fold increase in V_h. Using V_h as a measure of V_{blob} suggests that V_{blob} for CoE−PS is 1.9 times larger than for CoA−PS.[39] The difference in R_h is 3.8 Å, very close to the longest carbon-to-carbon distance found for toluene to equal 4.3 Å by using the molecular modeling software package HyperChem 7.02. This 4.3 Å distance represents the extra length separating pyrene from the CoE−PS backbone with respect to CoA−PS (Scheme 1). Consequently, these results suggest that the larger N_{blob} value obtained for CoE−PS is due in part to the longer linker between pyrene and the main chain, enabling pyrene to probe a larger V_{blob} in solution.

According to the definition of k_{blob} given in eq 7, the trends obtained for k_{blob} (Figure 5) and N_{blob} (Figure 9) are somewhat contradictory. Indeed, the above discussion indicates that a larger N_{blob} for the CoE−PS series implies a larger V_{blob}, which should result in a smaller k_{blob} for CoE−PS than for CoA−PS according to eq 7. Instead, the opposite effect is observed in Figure 5 with k_{blob}^{CoE-PS} being 1.4 times larger than k_{blob}^{CoA-PS} over the entire range of pyrene content. The reason for this discrepancy lays in the erroneous assumption being implicitly made that k_{diff} in eq 7 is not affected by the linker connecting pyrene to the backbone. Indeed, combining eq 7 with the fact that $k_{blob}^{CoE-PS} = 1.4 \times k_{blob}^{CoA-PS}$ and $V_{blob}^{CoE-PS} = 1.9 \times V_{blob}^{CoA-PS}$ implies that $k_{diff}^{CoE-PS} = 2.7 \times k_{diff}^{CoA-PS}$. In other words, the longer and more flexible ether linker of CoE−PS results in faster dynamics for excimer formation.

The differences in k_{diff} values can be rationalized by considering that the diffusional encounters between two pyrenes attached onto a polymer occur in a sequence of two steps as shown in Scheme 2. In the first step, the two polymer units bearing the pyrenes diffuse slowly toward each other with a forward (k_1) and backward (k_{-1}) reaction rate constant. In the second step, the pyrenes probe their nearby environment to form the excimer with a forward (k_2) and backward (k_{-2}) reaction rate constant. For the formation of pyrene excimer, the dissociation rate constant k_{-2} is usually negligible[4,5,11] so that k_{diff} can be approximated by eq 9.

$$k_{diff} = \frac{k_1 \times k_2}{k_{-1} + k_2} \tag{9}$$

In eq 9, k_1 and k_{-1} depend solely on the polymer backbone whereas k_2 depends on the linker. According to eq 9, the largest value taken by k_{diff} is k_1 which is observed only if $k_{-1} \ll k_2$, i.e. when the pyrenyl pendants rearrange themselves much more rapidly than two polymer units have time to diffuse away from one another. These conditions might be fulfilled for the CoE−PS samples where the longer and more flexible linker provides enough freedom of motion to the pyrenyl pendants. They are certainly much less likely to be fulfilled for the CoA−PS series

Scheme 2. Effect of Backbone and Side Chain Motion on the Kinetics of Excimer Formation

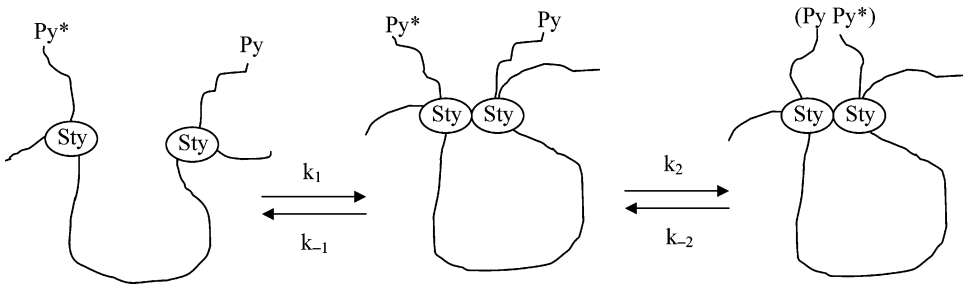

where the short and rigid amid linker reduces the mobility of the pyrenyl pendant, resulting in a k_{diff} value smaller than k_1. Switching from the rigid amide linker of CoA−PS to the flexible ether linker of CoE−PS seems to result in a 2.7 fold reduction of k_{diff}, a substantial slow down of pyrene mobility and decrease in excimer formation as observed in Figures 2 and 4.

(3) Effect of the Distribution of Pyrene Pendants. Interestingly, the monomer fluorescence decays of ES−PS where the pyrenes are spaced evenly along the backbone are very different from those of the randomly labeled polymer, CoA−PS (Figure 3). Instead of the complicated, multiexponential decays obtained for CoA−PS, the ES−PS decays are biexponential and nearly monoexponential in the 1.2 and 2.2 mol % labeling cases. Although the pyrenes of ES−PS are evenly spaced in 1-dimension, the random coil conformation of the polymer in solution is expected to produce a distribution of distances between pyrene labels resulting in a fluorescence decay more complicated and similar to that of a randomly labeled polymer. Such an example has been reported by Winnik et al. using an evenly spaced pyrene labeled polystyrene.[6]

In this work, the ES−PS monomer decays become slightly more complicated—less monoexponential—as the pyrene content increased from 1.2 up to 3.2 mol %. This is illustrated in the polydispersity (PDI) of the decays found in Table SI.3. Similar to the PDI used for describing the molecular weight distribution of polymers, a PDI can be defined for the fluorescence decays by taking the ratio τ_W/τ_N, where τ_N and τ_W are the number-average and weight-average lifetimes, respectively. The PDI of the decays increases from 1.05 to 1.16 for ES−PS and 1.27−1.40 for CoA−PS in the same pyrene content range of ∼1.1−3.5 mol %. Much larger PDIs were obtained for CoE−PS and GrE−PS. The more pronounced monoexponential character of the ES−PS decays suggests that excimer formation occurs via a single rate constant, i.e., that the pyrenes distribute themselves much more evenly in the ES−PS coil than in the polymer coil of any of the other Py−PS samples.

The even distribution of pyrene along the ES−PS chain has an interesting effect on the blob model parameters k_{blob} and k_e[blob]. To date, k_{blob} has always been greater than k_e[blob] for all polymers randomly labeled with pyrene that have been studied using the FBM. This was the case with GrE−PS, CoE−PS, and CoA−PS, as well as with Py−PDMA[19,25] and pyrene labeled poly(L-glutamic acid).[26] k_{blob} being greater than k_e[blob] implies that a ground-state pyrene located inside a blob is more likely to quench an excited pyrene than to diffuse out of the blob. However, the ES−PS series has k_{blob} and k_e[blob] values that are almost identical, indicating that ground-state pyrenes are just as likely to diffuse away as they are to remain inside a blob and quench the excited pyrene. This observation suggests that the pyrene labels are not only evenly spaced in one dimension but also evenly distributed in three dimensions inside the polymer coil. This conclusion is in agreement with the absence of curvature found in the monomer decays (Figure 3) which suggests that excimer formation can be described by a single rate constant. This unusual distribution also has an effect on $\langle n \rangle$, resulting in a much lower value than that of CoA−PS (Figure 6). Since pyrene appears to not distribute itself in the polymer coil of the ES−PS series according to the Poisson distribution usually encountered with randomly labeled polymers,[5] further comparisons of the FBM parameters between the CoA−PS and ES−PS series should be made with caution.

Conclusions

(1) Using the FBM To Describe Excimer Formation for Pyrene-Labeled Polymers. The experiments conducted in this study have demonstrated (1) how sensitive excimer formation is to the method of pyrene attachment and (2) how a rational for the trends shown in Figures 2 and 4 can only be obtained through a quantitative analysis of the pyrene monomer and excimer fluorescence decays. Presently, the FBM is the best suited tool to carry out this task.

Despite the resemblance in chemical structure and pyrene content of those four Py−PS series (Scheme 1), all Py−PSs showed major differences in excimer formation. Qualitative analysis of the fluorescence data using the ratio I_E/I_M (Figure 2) and the excimer formation rate constant k_{exci} (Figure 4) indicates that the long and flexible ether linker of GrE−PS and CoE−PS favors excimer formation. Excimer formation is reduced first when the linker is made shorter and stiffer (CoA−PS) and second, when the pyrene pendants are kept apart from one another (ES−PS). Quantitative analysis of the fluorescence decays using the FBM demonstrates that the long and flexible ether linker of GrE−PS and CoE−PS enables pyrene to probe a larger volume inside the polymer coil (Figure 9). The difference in volume probed by a pyrene between CoE−PS and CoA−PS is compatible with the length difference between the amide and ether linkers found by molecular modeling.

(2) Distribution of Modifications. The physical properties of homopolymers are often modified by covalently incorporating a molecule B into a homopolymer (polyA).[41,42] Most sought after modifications use a molecule B whose properties are very different from those of polyA. For example, the covalent attachment of a hydrophobic B molecule onto a water-soluble polyA results in a water-soluble associative thickener.[42] Interestingly, not only does the nature of the modification affect the behavior of the modified polymer, but so does the distribution of these modifications along the chain.[43,44] The inherent sensitivity limits set by most analytical techniques make it very difficult to gain more information about these modifications beyond the typical modification content of a modified polymer. The experiments conducted in this study demonstrate that by selectively labeling the modifications made to a polymer with pyrene (cf. ES−PS and CoA−PS which share a same linker to connect pyrene to the PS backbone), information on the fraction

of aggregated pyrene labels and, consequently, the level of clustering of the modifications is obtained through the parameter f_{agg}. As expected from the design of ES−PS, f_{agg} was found to be much smaller for ES−PS than for CoA−PS (Figure 10). These results validate the use of f_{agg} to determine the level of clustering of the modifications made to a polymer, as has been done earlier to determine the clustering of succinic anhydride pendants along maleated ethylene−propylene random copolymers[29,44] as well as the level of association of water-soluble associative thickeners.[19,23,28]

Analysis of the fluorescence decays acquired for the two Py−PSs obtained by copolymerization (CoA−PS and CoE−PS) resulted in similar f_{agg} values. Interestingly, GrE−PS and CoE−PS which have identical chemical structure do not yield similar f_{agg} values. The pyrene pendants appear to be more clustered in GrE−PS. It remains to be seen whether this observation can be generalized to other polymeric backbones.

(3) Protein Folding. Proteins are polypeptides where the distribution of pendants along the backbone is defined exactly by the 1-dimensional sequence of their gene. The early stages of protein folding are believed to involve the random diffusion-controlled encounters of the amino acids (aa's) constituting the protein.[45] These encounters lead to the intramolecular associations of some aa's into nuclei from which the nascent secondary structures of the folded protein originate. If the polypeptide is initially in a random coil conformation, the perfectly aligned aa's in the 1-dimensional sequence of the protein are expected to distribute themselves randomly in the 3-dimensional polypeptide coil. The random positioning of the aa's inside the polymer coil would be expected to result in random encounters between aa's which are no longer influenced by the specific location of the aa's along the chain. However this expectation is not supported by a comparison of the trends obtained in Figures 2 and 4 between ES−PS where the pyrenes are located at specific positions along the chain and CoA−PS where the pyrenes are randomly incorporated into the chain. For a same pyrene content, much fewer encounters were observed for ES−PS than for CoA−PS. This observation confirms that the exact positioning of the aa's along the polymer chain also controls the rate at which aa's encounter in the polypeptide coil, an information which might have some relevance for the study of the early stages of protein folding.

Acknowledgment. M.I. and J.D. acknowledge financial support from an Ontario's Premier Research Excellence Award and NSERC. J.D. is indebted to the CFI funding associated with his Tier-2 CRC award.

Supporting Information Available: Figure SI.1, I_E/I_M ratios as a function of pyrene content, Figure SI.2, k_{exci} as a function of pyrene content, Figures SI.3 and SI.4, monomer (left) and excimer (right) fluorescence decays, Table SI.1, molecular weights of the GrE−PS, CoA−PS, CoE−PS, and ES−PS series, Table SI.2, molecular weights of the high molecular weight fractions of the CoA−PS, CoE−PS, and ES−PS series, Table SI.3, parameters retrieved from the multi-exponential fits of the monomer decays of PyPSs, Table SI.4, parameters retrieved from the multi-exponential fits of the excimer decays of PyPSs, Tables SI.5 and SI.6, parameters retrieved from the global FBM analysis of the monomer decays of GrE−PS, CoE−PS, and CoA−PS, Table SI.7, fractions of all pyrene species for GrE−PS, CoE−PS, and CoA−PS, Table SI.8, parameters retrieved from the global FBM analysis of the monomer decays of ES−PSs, Table SI.9, parameters retrieved from the global FBM analysis of the excimer decays of ES−PSs, Table SI.10, fractions of all pyrene species for ES−PS, Table SI.11, monomer conversions from 1H NMR and I_E/I_M ratios measured with the GPC on-line fluorometer, Table SI.12, lifetimes retrieved from low labeled polymers and monomer compounds in THF, Table SI.13, slopes and errors for trend lines in Figures 4 and 8, Table SI.14, reproducibility of the I_E/I_M ratios and effect of the excitation wavelength, and Table SI.15, reproducibility of the average monomer lifetime. This material is available free of charge via the Internet at http://pubs.acs.org.

References and Notes

(1) Cuniberti, C.; Perico, A. *Eur. Polym. J.* **1977**, *13*, 369−374.
(2) Perico, A.; Cuniberti, C. *J. Polym. Sci.*: *Polym. Phys. Ed.* **1977**, *15*, 1435−1450.
(3) Winnik, M. A.; Redpath, T.; Richards, D. H. *Macromolecules* **1980**, *13*, 328−335.
(4) Winnik, M. A. *Acc. Chem. Res.* **1985**, *18*, 73−79.
(5) Duhamel, J. *Acc. Chem. Res.* **2006**, *39*, 953−960.
(6) Winnik, M. A.; Li, X.-B.; Guillet, J. E. *Macromolecules* **1984**, *17*, 699−702.
(7) Martinho, J. M. G.; Winnik, M. A. *Macromolecules* **1986**, *19*, 2281−2284.
(8) Picarra, S.; Duhamel, J.; Fedorov, A.; Martinho, J. M. G. *J. Phys. Chem. B* **2004**, *108*, 12009−12015.
(9) Winnik, F. M. *Chem. Rev.* **1993**, *93*, 587−614.
(10) Duhamel, J. In *Molecular Interfacial Phenomena of Polymers and Biopolymers*; Chen, P., Ed.; Woodhead Publishing Company: Cambridge, U.K., 2005, pp 214−248.
(11) Birks, J. B. *Photophysics of Aromatic Molecules*; Wiley: New York, 1970, p 301.
(12) Ezzell, S. A.; Hoyle, C. E.; Creed, C. E.; McCormick, C. L. *Macromolecules* **1992**, *25*, 1887−1895.
(13) Anghel, D. A.; Alderson, V.; Winnik, F. M.; Mizusaki, M.; Morishima, Y. *Polymer* **1998**, *39*, 3035−3044.
(14) Farinha, J. P. S.; Martinho, J. M. G.; Xu, H.; Winnik, M. A.; Quirk, R. P. *J. Polym. Sci., Part B*: *Polym. Phys.* **1994**, *32*, 1635−1642.
(15) Cuniberti, C.; Perico, A. *Eur. Polym. J.* **1980**, *16*, 887−893.
(16) Wang, F. W.; Lowry, R. E.; Cavanagh, R. R. *Polymer* **1985**, *26*, 1657−1660.
(17) Seixas de Melo, J.; Costa, T.; Miguel, M. da. G.; Lindman, B.; Schillen, K. *J. Phys. Chem. B* **2003**, *107*, 12605−12621.
(18) Mathew, A. K.; Siu, H.; Duhamel, J. *Macromolecules* **1999**, *32*, 7100−7108.
(19) Kanagalingam, S.; Ngan, C. F.; Duhamel, J. *Macromolecules* **2002**, *35*, 8560−8570.
(20) Braun, D.; Czerwinski, W.; Disselhoff, G.; Tudos, F.; Kelen, T.; Turcanyi, B. *Makromol. Chem.* **1984**, *125*, 161−205.
(21) Leoni, A.; Franco, S.; Saini, G. *Makromol. Chem.* **1973**, *165*, 97−104.
(22) James, D. R.; Demmer, D. R. M.; Verrall, R. E.; Steer, R. P. *Rev. Sci. Instrum.* **1983**, *54*, 1121−1130.
(23) Siu, H.; Duhamel, J. *Macromolecules* **2004**, *37*, 9287−9289.
(24) Tachiya, M. *Chem. Phys. Lett.* **1975**, *33*, 289−292.
(25) Kanagalingam, S.; Spartalis, J.; Cao, T.-M.; Duhamel, J. *Macromolecules* **2002**, *35*, 8571−8577.
(26) Duhamel, J.; Kanagalingam, S.; O'Brien, T.; Ingratta, M. *J. Am. Chem. Soc.* **2003**, *125*, 12810−12822.
(27) Prazeres, T. J. V.; Beingessner, R.; Duhamel, J.; Olesen, K.; Shay, G.; Bassett, D. R. *Macromolecules* **2001**, *34*, 7876−7884.
(28) Siu, H.; Duhamel, J. *Macromolecules* **2006**, *39*, 1144−1155.
(29) Zhang, M.; Duhamel, J. *Macromolecules* **2005**, *38*, 4438−4446.
(30) Press, W. H.; Flannery, B. P.; Teukolsky, S. A.; Vetterling, W. T. *Numerical Recipes. The Art of Scientific Computing (Fortran Version)*; Cambridge University Press: Cambridge, U.K., 1992.
(31) Demas, J. N. *Excited-State Lifetime Measurements*; Academic Press: New York, 1983.
(32) Winnik, M. A.; Egan, L. S.; Tencer, M.; Croucher, M. D. *Polymer* **1987**, *28*, 1553−1560.
(33) Siu, H.; Duhamel, J. *Macromolecules* **2005**, *38*, 7184−7186.
(34) Anghel, D. F.; Toca-Herrera, J. L.; Winnik, F. M.; Rettig, W.; v. Kliting, R. *Langmuir* **2002**, *18*, 5600−5606.
(35) Winnik, F. M.; Regismond, S. T. A.; Goddard, E. D. *Langmuir* **1997**, *13*, 111−114.
(36) Flory, P. J. *Principles of Polymer Chemistry*; Cornell University Press: Ithaca, NY, 1953, p 598.
(37) Gauthier, M.; Möller, M. *Macromolecules* **1991**, *24*, 4548−4553.
(38) Bandrup, J.; Immergut, E. H.; Grulke, E. A. *Polymer Handbook*, 4th ed.; John Wiley & Sons: New York, 1999; pp VII 675−683.
(39) A similar conclusion can be reached by using scaling arguments[40] and noting that $V_{blob} \propto N_{blob}^{3\nu}$ where ν is the Flory exponent equal to 0.6 for PS in THF.

(40) de Gennes, P.-G. *Scaling Concepts in Polymer Physics*; Cornell University Press: Ithaca, NY, 1979.
(41) Jao, T. C.; Passut, C. A. In *Handbook of Detergents, Part D: Formulation*; Showell, M. S., Ed.; CRC Press, Taylor and Francis Group: Boca Raton, FL, 2006; pp 437−471.
(42) Winnik, M. A.; Yekta, A. *Curr. Opin. Colloid Interface Sci.* **1997**, *2*, 424−436.
(43) Volpert, E.; Selb, J.; Candau, F. *Macromolecules* **1996**, *29*, 1452−1463.
(44) Zhang, M.; Duhamel, J.; van Duin, M.; Meessen, P. *Macromolecules* **2004**, *37*, 1877−1890.
(45) Karplus, M.; Weaver, D. L. *Nature (London)* **1976**, *260*, 404−406.

MA070368H